Accepted Manuscript

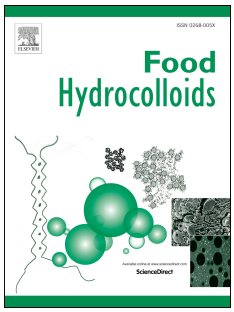

Multi-scale structure, pasting and digestibility of adlay (*Coixlachryma-jobi L.*) seed starch

Jicheng Chen, Yazhen Chen, Huifang Ge, Chunhua Wu, Jie Pang, Song Miao

PII: S0268-005X(18)31522-4

DOI: https://doi.org/10.1016/j.foodhyd.2018.11.050

Reference: FOOHYD 4791

To appear in: *Food Hydrocolloids*

Received Date: 13 August 2018

Revised Date: 27 November 2018

Accepted Date: 27 November 2018

Please cite this article as: Chen, J., Chen, Y., Ge, H., Wu, C., Pang, J., Miao, S., Multi-scale structure, pasting and digestibility of adlay (*Coixlachryma-jobi L.*) seed starch, *Food Hydrocolloids* (2018), doi: https://doi.org/10.1016/j.foodhyd.2018.11.050.

This is a PDF file of an unedited manuscript that has been accepted for publication. As a service to our customers we are providing this early version of the manuscript. The manuscript will undergo copyediting, typesetting, and review of the resulting proof before it is published in its final form. Please note that during the production process errors may be discovered which could affect the content, and all legal disclaimers that apply to the journal pertain.

View metadata, citation and similar papers at core.ac.uk

brought to you by CORE

provided by T-Stor

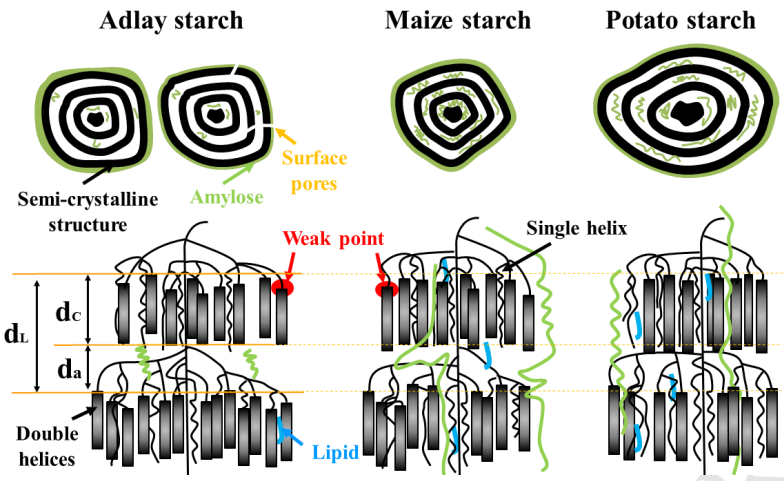

ACCEPTED MANUSCRIPT

ACCEPTED MANUSCRIPT

Multi-scale structure, pasting and digestibility of Adlay (*Coixlachryma-jobi L.*) seed starch

Jicheng Chen[1,2], Yazhen Chen[2], Huifang Ge[2], Chunhua Wu[2], Jie Pang[2], Song Miao[1,3,2]*

[1]*China-Ireland International Cooperation Center for Food Material Science and Structure Design, Fujian Agriculture and Forestry University, Fuzhou, China*

[2]*College of Food Science, Fujian Agriculture and Forestry University, Fuzhou,China*

[3]*Teagasc Food Research Centre, Moorepark, Fermoy, Co. Cork, Ireland*

*****Corresponding author.

Dr. Song Miao

Tel: +353 2542468

Fax: +353 2542340

E-mail: song.miao@teagasc.ie

ACCEPTED MANUSCRIPT

Abstract: The hierarchical structure, pasting and digestibility of adlay seed starch (ASS) were investigated compared with maize starch (MS) and potato starch (PS). ASS exhibited round or polyglonal morphology with apparent pores/channels on the surface. It had a lower amylose content, a looser and more heterogeneous C-type crystalline structure, a higher crystallinity, and a thinner crystalline lamellae. Accordingly, ASS showed a higher slowly digestible starch content combined with less resistant starch fractions, and a decreased pasting temperature, a weakened tendency to retrogradation and an increased pasting stability compared with those of MS and PS. The ASS structure-functionality relationship indicated that the amylose content, double helical orders, crystalline lamellar structure, and surface pinholes should be responsible for ASS specific functionalities including pasting behaviors and *in vitro* digestibility. ASS showed potential applications in health-promoting foods which required low rearrangement during storage and sustainable energy-providing starch fractions.

Keywords: Adlay seed starch; multi-scales structures; pasting properties; digestibility

ACCEPTED MANUSCRIPT

1. Introduction

Adlay (*Coixlachryma-jobi L. var. ma-yuenStapf*), commonly known as adlay or Job's tears, is an annual crop widely cultivated in East and South-East Asia (Chaisiricharoenkul, Tongta, & Intarapichet, 2011; Chang, Huang, & Hung, 2003). Adlay seeds contain a great number of health-beneficial bioactive components (e.g., protein, polysaccharide, polyphenols, coixenolide, coixol, oil, etc.) and have been considered as a traditional oriental medicine for centuries for the treatment of edema, rheumatism, and neuralgia (Liu et al., 2017; Tseng, Yang, Chang, Lee, & Mau, 2006; Zhu, 2017). Besides, numerous studies have been reported that adlay seeds have the ability to prevent the formation of tumors, reduce inflammation, ameliorate metabolic syndrome, and aid in gastrointestinal tract regulation (Chen, Lo, & Chiang, 2012; Tsai, Yang, & Hsu, 1999; Wenchang, Cheng, Mengtsan, & Kingthom, 2000). Owing to its perceived nutritional and health benefits, adlay seeds are increasingly utilized in the food industry.

The major component of adlay seeds is starch, accounting for approximately 54.26%-58.15% of its dry mater (Chaisiricharoenkul et al., 2011; Liu, Han, & Sun, 2012). Over the last decade, adlay seed starch (ASS) has been served as a food ingredient through several food products such as baked products, soups, broths, distilled liquor, etc. (Yang, Peng, Lui, & Lin, 2008; Zhu, 2017) . Besides, the relationships between supramolecular structures and pasting features of adlay seed starches have been revealed (Miao et al., 2018; Xu et al., 2017). However, studies focused on ASS physicochemical properties and functionalities such as the content of rapidly digestible starch (RDS), slowly digestible starch (SDS), and resistant starch (RS) are scarce (Chaisiricharoenkul et al., 2011; Li & Corke, 1999). Importantly, long-term consumption of starchy foods enriched with RDS was regarded as a

fundamental cause to a wide variety of metabolic complications such as obesity and type II diabetes (Brandmiller, Dickinson, Barclay, Celermajer, 2007; Brandmiller, 2007).

The SDS fractions which provide a slow and prolonged release of glucose, and the RS that cannot be digested in human upper gastrointestinal tract but is used by microflora in the colon are more than encouraged for a health-promoting diet (Lehmann & Robin, 2007). With a never growing population and human health interests, there could be a shortage of common health-promoting starches for industrial food applications in the future. Therefore, it is essential to identify, characterize and use non-conventional starches for industrial applications. Based on the excellent functionalities of adlay, further insights into the ASS multi-scale structure and functionalities such as pasting properties and digestibility are inevitable and necessary.

Although most native starches are semi-crystalline (containing crystalline and amorphous lamellae) in nature, their granule size, shape and microstructures are diverse, depending on their botanical source, growing and harvesting conditions (Liu et al., 2017). The granule size of starches ranged from 1.5 μm to 100 μm, while the shape varied from irregular to elliptical, tetrahedral, polygonal and spherical forms. And the hierarchical structures of starch granules have been confirmed to be the critical determinant of starch functionalities for food processing and human nutrition (Chi et al., 2017). Thus, understanding the relationships between hierarchical structures and functional properties (e.g. digestibility and pasting properties) of starch is very important for optimizing food and industrial applications (Syahariza, Sar, Hasjim, Tizzotti, & Gilbert, 2013) .

The aim of this study was to investigate the physicochemical, micro-structural, thermal, pasting and digestibility properties of ASS. The relationships of structures and functionalities of ASS were also discussed to state whether the ASS is suitable for the health-promoting foods or other specific industrial applications. The results were compared with commercial maize starch (MS) and potato starch (PS). This study will provide a scientific basis to extend the commercial applications of ASS.

2. Materials and Methods

2.1. Materials

The adlay was planted in May and harvested in December in Pucheng, the county of FuJian in China. The county showed an average temperature of 17.4 °C, annual rainfall of 1780 mm, and annual sunshine time of 1893 h.

Commercial potato and maize starch were purchased from Kang yuan Co., Ltd, (Henan, China) and used for comparison with ASS. Pancreatin from porcine pancreas and amyloglucosidase were purchased from Sigma-Aldrich Co., Ltd. The D-glucose assay kit (GOPOD, K-GLUC) was purchased from Megazyme International Ireland Co., Ltd. (Wicklow, Ireland). All chemical reagents were of analytical reagent grade. Commercial starches and chemicals were used directly without further purification.

2.2. Isolation of ASS

Starch was isolated from adlay seeds following the previously published methods with some modifications (Kim et al., 2008). The seeds were steeped in excess water for 4 h at 25 °C, grounded in an organization broking machine (JJ-2B, Four Red Instrument, Co., Ltd., Shanghai, China) at full speed for 1 min and filtered through 200-mesh sieves. The NaOH (0.05g/L) was added into the filtrate, with stirring for 10 min and then after stewing for 3 h at 25 °C, the supernatant and the top, yellowish layer

of protein was removed. The sediment was washed several times with deionized water. The ethanol and diethyl ether were added to the starch suspension to eliminate non-starch polysaccharide and lipid. Then the starch suspension was centrifuged at 5000×*g* for 10 min. After centrifugation, the supernatant and dark tailing layer were discarded and the residue was washed several times with deionized water until the supernatant was clear. Then the residue was dried at 40 °C and milled below 50 °C to yield the starch and stored in a sealed plastic bag.

2.3. Chemical Composition Analysis of starches

The starch content, moisture, protein, lipid and ash of starch were determined by the standard methods of AOAC (Scott & Helrich, 1990) procedures. The amylose contents were determined by the method of iodine colorimeter at 620 nm using a potato starch standard mixture (Yu, Ma, Menager, & Sun, 2012) . The results were reported on a dry weight basis. All the experiments were performed at least in triplicate and results were presented as the mean value.

2.4. Crystal structure analysis

The crystal structure of starches was determined with an Xpert PRO diffractometer (Rigaku, Corp., Tokyo, Japan), operated at 40 mA and 40 kV with an X-ray source of Cu Kα radiation (λ= 0.1542 nm). The range of the diffraction angle (2θ) was from 5° to 60° with a scanning speed of 10°/min and scanning step of 0.033°. The moisture content of each sample was equilibrated at 40 °C and all were approximately 10%. The crystallinity of starch was calculated by following equation:

$$Crystallinity(\%) = \frac{A_C}{A_C + A_a} \times 100$$

where A_c is the crystalline area and A_a is amorphous on the X-ray diffractogram.

2.5. Lamellar structure

Lamellar structure of starches was detected by a synchrotron small angle X-ray scattering (SAXS) system at Shanghai Synchrotron Radiation Facility (SSRF, China). A monochromatic beam of 0.124 nm was used and the sample-to-detector distance was 1860 mm, which provided a q-range from 0.10 to 1.5 nm^{-1}. Samples were presented in 2 mm sealed quartz capillaries as suspensions containing excess water and scattering was measured for 60 s. A sealed 2 mm quartz capillary filled with water was used as a background. SAXS curves were normalized to sample transmission and background-subtracted using fit 2D software. The Bragg spacing d, i.e. the thickness of starch lamellar structure, was calculated from the position of the peak (q) according to $d=2\pi/q$.

In order to further clarify the structural parameters of semi-crystalline lamellae, one-dimensional correlation function profiles were calculated according to following equation (Chi et al., 2017; Kuang et al., 2017):

$$f(r)=\frac{\int_0^\infty I(q)q^2\cos(qr)dq}{\int_0^\infty I(q)q^2dq}$$

where r represents the distance in real space.

2.6. Morphology observation and particle size analysis

Granule micrographs were observed at 3000 × magnification under a scanning electron microscope (XL30, Philips, Holand), and the light property of granule were observed viewed under the Olympus BX53 polarized light microscope according to the method of Man et al. (2012). The granule size analysis carried out with JEDA-801D particle size analyzer (Jiangsu JEDA Science-Technology Development Co., Ltd., Nanjing, China).

2.7. Gelatinization properties

The gelatinization properties of the samples were studied by using a differential scanning calorimeter (DSC-200F3 NETZSCH-Gerätebau GmbH, Germany). Indium was used as the calibration standard. Starch slurries were prepared at 1:3 dry starch/ratios and sealed, reweighed. Samples then were allowed to heat from 10 °C to 110 °C at a heating rate of 10 °C per minute. The onset temperature (T_o), peak temperature (T_p), conclusion temperature (T_c), gelatinization temperature range (T_c-T_o) temperatures, as well as enthalpy (ΔH_{gel}), were calculated. All thermal analyses were conducted in triplicate for each starch.

2.8. Pasting properties

The pasting properties of starches were analyzed by using Brabender Visco-Analyser (Brabendviscograph-E, Brabender GmbH & Co. KG, Germany). Briefly, the starch sample (8% w/w, d.b.) were subjected to the following heating and cooling program: equilibrated at 35 °C for 5 min, heated to 95 °C in 40 min, held at 95 °C for 30 min, cooled to 50 °C in 40 min, and held at 50 °C for 30 min. All measurements were performed in triplicate.

2.9. *In vitro* starch digestibility

In vitro starch digestibility was analyzed according to the Englyst method (Englyst, Kingman, & Cummings, 1992) with slight modifications. Enzyme working solution containing 780 USP porcine pancreatin and 3 units amyloglucosidase was freshly prepared before use. Starches (1.0 g, dsb) were dispersed in 20.0 mL acetate buffer solution (0.1 M, pH 5.2) with 4 mM $CaCl_2$, then six glass balls were added to the starch suspension and incubated with 5mL enzyme solution under continuous shaking (190 rpm) at 37 °C. An aliquot (0.5 mL) of the hydrolysate was removed at

time intervals of 20 min and 120 min, and then mixed with 20 mL 70% ethanol to denature the enzymes. The samples were centrifuged at 5000×*g* for 5 min and the glucose content in the supernatant was measured with the Megazyme glucose assay kit (GOPOD method). The glucose content at intervals of 20 and 120 min was labeled as G20 and G120, and the contents of rapidly digestible starch (RDS), slowly digestible starch (SDS) and resistant starch (RS) content were calculated by the following equations:

$$RDS=G20\times0.9/TS\times100\%$$

$$SDS=(G120-G20)\times0.9/TS\times100\%$$

$$RS=[TS-RDS-SDS]/TS\times100\%$$

where the TS means the total starch (TS) content of the complexes used for digestibility measurement. Herein, the TS equals to 1 g.

2.10. Statistical analysis

One-way analysis of variance (ANOVA) was performed with Tukey's HSD test ($^{*}p<0.05$) using SPSS (20.0 version, IBM). The significance level was set as $^{*}p< 0.05$.

3. Results and Discussion

3.1. Proximate composition analysis of ASS

The chemical components of starches are presented in Table S1. The starch content of adlay seed (yield of (43.2 ± 0.13)%, d.b.s) is lower than that extracted from adlay seed planted in Japan, Burma and Thailand (Wu, Charles, & Huang, 2007), which may be attributed to the variation in different cultivation climates and regions. Careful isolation and washing procedures resulted in clean ASS (the purity reached 97.54±0.61%). The range of moisture contents in these starches varied from 7.74% to

9.37%. ASS showed slightly higher moisture content (8.10±0.17) % than maize starch (7.74±0.06%). The residual protein and lipid contents of ASS were (0.38 ± 0.05) % and (0.07 ± 0.01) %, respectively, which is lower than that of MS and PS, indicating protein and lipid are extracted extensively from ASS. The ash contents of ASS, potato starch and maize starch are (0.14± 0.01) %, (0.20±0.04) % and (0.19± 0.03) %, respectively.

The amylose content of these starches ranged from 2.25 to 24.60%. It was observed that the amylose content (2.25±0.76%) of ASS was much lower than that of potato starch (23.32±0.42%) and maize starch (24.60±0.25%), respectively. The amylose content of ASS is considerably different to published data in a previous literature (Li et al., 1999), i.e., the amylose content of normal ASS and waxy ASS is 15.9%-25.8% and 0.7%-1.1% respectively. These results indicated that the physicochemical properties of ASS maybe significantly different to other cereal starches.

3.2. Crystal propertiesof starches

X-ray diffraction patterns of ASS, MS, and PS are shown in Fig.1. The MS and PS displayed typical A- and B-type patterns, respectively. It can be seen that ASS exhibited diffraction peaks at 5.6 º, 15.2 º, 17.2º, 18.4º and 23.6º (*2θ*), suggesting that ASS showed a C-type (hybrid of A-type and B-type) X-ray pattern (Man et al., 2012). This observation was consistent with the result reported by a previous literature (Kim et al., 2008). The degree of crystallization of ASS was 35.79% (Table 1), which was higher than that of PS (29.83%) and MS (31.25%). ASS contained a vast number of branched short chains, which was more readily packed into double helices and arranged to form starch crystals. Therefore, ASS had the highest degree of crystallization which follows the orders of ASS > MS > PS. According to previous studies (Chi et al., 2017; Lopez-Rubio, Flanagan, Shrestha, Gidley, & Gilbert, 2008),

starch crystalline structures, especially the crystallinity, were significantly related to starch gelatinization properties, pasting behaviors and digestibility. Understanding crystalline structures would be of help to accelerate ASS-based food development and applications.

3.3. Lamellar structure of starches

As the alternating stack of amorphous and crystalline regions, semi-crystalline lamellae assembled with a repeat distance of 9-10 nm. A characteristic peak at approximately 0.6 nm^{-1} was observed for all starches from Fig.2, indicating the existence of starch semi-crystalline lamellae. To be more accurate, ASS had a peak at 0.6624 nm^{-1} and PS, MS showed peaks at 0.6503 and 0.6528 nm^{-1}, respectively, corresponding to the Bragg distances of 9.48, 9.83 and 9.62 nm calculated from Woolf-Bragg's equation ($d=2\pi/q$) (Table 1). Starch lamellar thickness was highly associated with the susceptibility of enzymes attack and hydrothermal treatment (Wang et al., 2018). To further understand the characteristics of starch lamellar structures such as the thickness of crystalline lamella (d_c), amorphous lamella (d_a) and long repeated distance ($d_L=d_a+d_c$), the one-dimensional function profile was also used in this work (Fig. S1). Adopting the method, long repeated distance of semi-crystalline lamellae (d_L) can be calculated as the value of r at the second maximum of f(r), d_a is representing the solution of linear regression in the auto correlation triangle at f(r) = value of the flat minimum (Fig.S1). Hence, the average thickness of the crystalline lamellae d_c, equals to (d_L-d_a). As seen from Table 1, d_L showed similar changes to that of d and always showed a smaller value when calculated from Woolf-Bragg's equation. It could have resulted from the different starch model hypothesis (Fan et al., 2014), i.e., d value was obtained based on a paracrystalline model (the three-phase model which contained amorphous background, crystalline and amorphous phases)

and the d_L linear correlation function approach which only concerned the crystalline/amorphous phases. Notably, although ASS had smallest d or d_L, it possessed the largest d_a (2.99 nm), which was higher than that of PS (2.59 nm) and MS (2.84 nm). This observation could be attributed to the differences in the fine structure of amylose and amylopectin from different botanical origins.

3.4. Morphology and size distribution of starch granules

The scanning electron micrographs (SEM) and polarized light microscope (PLM) of MS, PS and ASS are presented in Fig.3. It can be seen that MS and ASS granules are round or polyglonal in shape with smooth surfaces (Fig.3a, e), while PS had a different morphology (oval or polyglonal) with larger granules (Fig.3b). According to the SEM photos, MS and PS did not showed any surface pinholes, while ASS apparently observed with channels or pinholes on granular surface. To our knowledge, channels always provide direct access of reagents to a loosely organized region at the hilum, which makes it possible to increase the accessibility of enzymes to starch (Buléon, Colonna, Planchot, & Ball, 1998). This observation indicated that the surface pinholes should be one of the critical factors determined the differential digestibility among MS, PS and ASS.

For starches with semi-crystalline granules, most of starch granules exhibited a Maltese cross under polarized light microscope (Sandhu, Singh, & Kaur, 2004) . The MS and ASS have typical Maltese cross in the central position (Fig.3a and c). However, the Maltese cross of PS is at one end of granule (Fig. 3b). It can also be seen that the size of PS is bigger than MS and ASS, which is in agreement with the scanning electron micrographs observed.

The size-distribution curves of starch granules are displayed in Fig.3g. It can be observed that ASS and MS showed similar uni-modal size distribution at 4-31 μm, but

the PS exhibit a wider uni-modal size distribution at 17-104 μm. The average particle sizes were 14.61 μm, 14.15 μm and 48.18 μm for ASS, MS and PS, respectively. The variation of starch granules may be attributed to the biological origin, biochemistry of the amyloplast or chloroplast, as well as the physiology of the plant (Man et al., 2012; Singh, Singh, Kaur, Sodhi, & Gill, 2003). Starch granules with smaller particle size are less resistant to the permeation of water/digestive enzymes into the granules, which would critically influence the starch pasting properties or digestibility (Tan et al., 2015; Zhang & Hamaker, 2009).

3.5. Gelatinization properties of starches

The gelatinization properties of starches were investigated by DSC. The endothermic gelatinization properties are displayed in Table 2. The ASS, MS and PS illustrate endothermic peaks between 60 and 85 °C. The transition temperatures (T_o, T_p, T_c) and ΔH_{gel} of starches from adlay seed, corn and potato starches were significantly different (Table 3). The T_o of ASS in water was slightly lower that of MS and PS. However, the T_p and T_c of ASS in water were higher than that of MS and PS, respectively. Broader gelatinization temperature ranges were observed (T_c-T_o) for ASS in comparison with that of MS or PS, which indicated the more heterogeneous crystalline structure of ASS. Generally, the orders of the starch double helices, size of crystallites and length of starch branch chain may contribute to these diverse views (Kim et al., 2008). Hence, ASS tends to have a looser double helices order, and thereby the ΔH_{gel} of ASS was lower than that of MS and PS, respectively. These observation might ascribe to the differences in the granular structure, amylose content, crystallinity and content or perfection of the double helices of starches (Singh et al., 2003; Xie, Liu, & Cui, 2006).

3.6. Pasting properties of starches

Starches from different plant sources exhibited their unique pasting behaviors, which were important for the evaluation and estimation of process design, unit operation and quality of the final starch products (Huang et al., 2014). The pasting profiles of three different starches were measured by Brabender viscometer and the parameters obtained from the pasting curve are listed in Table 3. Among the three starches, ASS had the lowest pasting temperature, which was in agreement with the DSC results. Moreover, ASS had the highest peak viscosities (1473.0 BU) and breakdown viscosities (1163.0 BU), but the lowest setback viscosities (395.0 BU), final viscosities (105.0 BU), and pasting temperatures (66.4 °C). The results indicated that the ASS is suitable for a long-time storage since its low retrogradation. Notably, the amylose content of ASS was negatively correlated to the peak and breakdown viscosities, but positively correlated to the setback viscosities, final viscosities, and pasting temperatures. These observations were well in accordance with the previous report that higher amylopectin contents resulted in a higher peak viscosity and lower setback viscosity (Ibanez et al., 2007). On the other hand, some researchers have reported that proteins and lipid influenced the pasting properties of rice starch and the forming of amylose-lipid complexes (Dautant, Simancas, Sandoval, & Muller, 2007; Marcoa & Rosell, 2008), which significantly affected the final viscosity, setback value, and pasting temperature of starch. In this work, lower lipid and protein content in ASS would contribute to the lower pasting temperature and higher breakdown viscosity.

3.7. *In vitro* digestibility of starches

Starch is the most important energy resource for humans, and the digestion behavior is critically related to human health. Depending on the rate and extent of

hydrolysis, starch fractions were classified as shown in Table 4. ASS had higher digestibility with less RS and higher RDS than those of MS and PS, indicating that ASS was likely to contribute to a higher glycemic response after ingestion. In addition, ASS showed higher SDS content than that of both MS and PS, suggesting ASS could provide more sustainable energy for the human body. Due to starch functionalities are highly correlated with its original multi-scale structures (Lopez-Rubio et al., 2008; Man et al., 2012; Wang et al., 2018), the differences in digestibility among ASS, MS and PS should be a result of the distinct hierarchical structures.

3.8. Mechanism of starch structural properties and functionalities

In starch granules, linear amylose and highly branched amylopectin are packed into the amorphous and crystalline starch regions with different length scales, including the molecular scale (~0.1 nm), lamellar structure (8-10 nm), growth rings (~0.1 μm), and whole granular morphology (1-100 μm) (Pikus, 2005; Zhang, Chen, Li, Li, & Zhang, 2015). These hierarchical structures always play key roles in starch functionalities, such as starch pasting properties and digestibility (Benmoussa, Moldenhauer, & Hamaker, 2007; Tan et al., 2015).

Schematic structural differences between ASS, MS and PS are illustrated in Fig. 4. ASS had smaller granular size and less amylose content entangled on the granular surface compared with MS and PS. Besides, ASS showed a more heterogeneous crystalline structure with thicker amorphous lamellae, thinner crystalline lamellae and semi-crystalline lamellae. The less amylose content and heterogeneous crystalline features should be responsible for the weaker resistance to hydrothermal treatment (Table 3). The lipids content within starch granules always contributed to a higher pasting temperature/gelatinization temperature, since lipids would interact with amylose or long-branched chains of amylopectin to form starch-lipid inclusion

346 complexes which had a high thermostability. ASS had much lower lipid content
347 (Table S1), which might significantly contribute to the lower pasting and
348 gelatinization temperatures (Table 3 and Table 4). Although ASS showed higher
349 crystallinity than those of MS and PS, a looser and more heterogeneous crystalline
350 structure as well as thinner crystalline lamellae contributed to its lower
351 thermostability. However, ASS showed lower setback viscosity than MS and PS,
352 which ascribed to the higher amylopectin content and the difficulty of amylopectin
353 rearrangement in a short timeframe. Actually, starch rearrangement and aging always
354 decreased food quality which in turn leading to a deterioration of consumer
355 acceptance. Therefore, ASS showed promising potential applications in the food
356 industry such as instant soups, sauces and jelly, due to its low retrogradation during
357 storage.

358 On the other hand, starch digestibility was critically related to human health and
359 was influenced by structural features. Amylose entangled at the starch granular
360 surface increased starch compactness, which could resist enzymes attack. In addition,
361 surface pores/channels on the starch granules also increased enzyme accessibility to
362 starches, since enzymes could enter starch interior through pores/channels. According
363 to a previous study (Jane, Wong, & McPherson, 1997), starch with a B type
364 crystalline structure had most of the branch points (i.e., α-1,6-glycosidic linkages)
365 clustered in the amorphous region and making them less susceptible to the enzymatic
366 hydrolysis, while A or C (A+B) type crystalline structure had ‘weak points’(i.e.,
367 susceptible to enzymatic hydrolysis) due to its branch points scattered in both
368 amorphous and crystalline regions. Therefore, ASS, a typical C type starch, had a
369 higher RDS content compared with PS. Generally, starch crystalline lamellae showed
370 a more compact structure than that of amorphous lamellae, and in turn, making the

amorphous lamellae is easily digested when enzymes were treated. ASS had a thinner crystalline lamellae and thicker amorphous lamellae than those of MS and PS, indicating ASS could be digested by enzymes such as α-amylase easily. Importantly, a looser and more heterogeneous crystalline structure of ASS also contributed to a higher susceptibility of starch to enzymes. Herein, ASS had a higher RDS content and a lower RS fraction compared with MS and PS. Nevertheless, ASS showed a higher crystallinity, which should be responsible for its higher SDS content than MS and PS.. It could be concluded that structural features such as amylose content, surface pores, crystalline structure and lamellar structures contributed to ASS digestion behaviors. ASS, which had a higher SDS content, could be used for health-promoting foods which required a slow and prolonged release of glucose.

4. Conclusions

In this work, ASS was extracted by alkaline steeping and it's physicochemical and functionalities were investigated in comparison with commercial MS and PS. Although the ASS used in this study cannot represent the starches from coix in China, the structural features and functionalities relationships of ASS from the ASS major planting area were revealed. ASS had low amylose content and apparent surface pores/channels. It exhibited relatively high crystallinity, but a loose and heterogeneous C type crystalline structure. In addition, ASS had a thicker amorphous lamellae and thinner crystalline lamellae. All these structural features contributed to ASS lower pasting temperature, lower setback viscosity, higher RDS content and higher SDS fractions compared with those of MS and PS. It can be concluded that ASS can be used as an addictive in health-promoting foods which required high stability during storage and are rich energy-providing starch fractions.

ACCEPTED MANUSCRIPT

Acknowledgments

The authors would like to thank the support of Development Project of Marine High-Tech Industry in Fujian Province (Min Hai Yu Gao Xin No. [2004] 03) and Project of High-level University Construction of Fujian Agriculture and Forestry University (No. 612014042).

ACCEPTED MANUSCRIPT

401 **References**

402 Benmoussa, M., Moldenhauer, K. A. K., & Hamaker, B. R. (2007). Rice Amylopectin
403 Fine Structure Variability Affects Starch Digestion Properties. *Journal of*
404 *Agricultural and Food Chemistry, 55*(4), 1475-1479.
405 http://dx.doi.org/10.1021/jf062349x.
406 Buléon, A., Colonna, P., Planchot, V., & Ball, S. (1998). Starch granules: structure and
407 biosynthesis. *International Journal of Biological Macromolecules, 23*(2),
408 85-112. http://dx.doi.org/10.1016/S0141-8130(98)00040-3.
409 Brandmiller J., Dickinson S., Barclay A., Celermajer D (2007). The glycemic index
410 and cardiovascular disease risk. *Current Atherosclerosis Reports, 9(6),*
411 479-485. http://dx.doi.org/10.1007/s11883-007-0064-x.
412 Brandmiller J (2007). The glycemic index as a measure of health and nutritional
413 quality: an Australian perspective. *Cereal Foods World, 52(2),* 41-44.
414 http://dx.doi.org/10.1007/s10900-012-9584-6.
415 Chaisiricharoenkul, J., Tongta, S., & Intarapichet, K.-O. (2011). Structure and
416 chemical and physicochemical properties of Job's tear (Coix lacryma-jobi L.)
417 kernels and flours. *Suranaree J. Sci. Technol, 18,* 109-122.
418 Chang, H. C., Huang, Y. C., & Hung, W. C. (2003). Antiproliferative and
419 chemopreventive effects of adlay seed on lung cancer in vitro and in vivo.
420 *Journal of Agricultural and Food Chemistry, 51*(12), 3656-3660.
421 http://dx.doi.org/10.1021/jf021142a.
422 Chen, H. J., Lo, Y. C., & Chiang, W. C. (2012). Inhibitory effects of adlay bran (Coix
423 lachryma-jobi L. var. ma-yuen Stapf) on chemical mediator release and
424 cytokine production in rat basophilic leukemia cells. *Journal of*
425 *Ethnopharmacology, 141*(1), 119-127.
426 http://dx.doi.org/10.1016/j.jep.2012.02.009.
427 Chi, C. D., Li, X. X., Zhang, Y. P., Chen, L., Li, L., & Wang, Z. J. (2017).
428 Digestibility and supramolecular structural changes of maize starch by
429 non-covalent interactions with gallic acid. *Food & Function, 8*(2), 720-730.
430 http://dx.doi.org/10.1039/c6fo01468b.
431 Dautant, F. J., Simancas, K., Sandoval, A. J., & Muller, A. J. (2007). Effect of
432 temperature, moisture and lipid content on the rheological properties of rice
433 flour. *Journal of Food Engineering, 78*(4), 1159-1166.
434 http://dx.doi.org/10.1016/j.jfoodeng.2005.12.028.
435 Englyst, H. N., Kingman, S., & Cummings, J. (1992). Classification and measurement
436 of nutritionally important starch fractions. *European Journal of Clinical*
437 *Nutrition, 46*, S33-50.
438 Fan, D., Wang, L., Chen, W., Ma, S., Ma, W., Liu, X., Zhao, J., & Zhang, H. (2014).
439 Effect of microwave on lamellar parameters of rice starch through small-angle
440 X-ray scattering. *Food Hydrocolloids, 35*, 620-626.
441 http://dx.doi.org/10.1016/j.foodhyd.2013.08.003.

Huang, J. R., Chen, Z. H., Xu, Y. L., Li, H. L., Liu, S. X., Yang, D. Q., & Schols, H. A. (2014). Comparison of waxy and normal potato starch remaining granules after chemical surface gelatinization: Pasting behavior and surface morphology. *Carbohydrate Polymers, 102*, 1001-1007. http://dx.doi.org/10.1016/j.carbpol.2013.07.086.

Ibanez, A. M., Wood, D. F., Yokoyama, W. H., Park, I. M., Tinoco, M. A., Hudson, C. A., McKenzie, K. S., & Shoemaker, C. F. (2007). Viscoelastic properties of waxy and nonwaxy rice flours, their fat and protein-free starch, and the microstructure of their cooked kernels. *Journal of Agricultural and Food Chemistry, 55*(16), 6761-6771. http://dx.doi.org/10.1021/jf070416x.

Jane, J. L., Wong, K. S., & McPherson, A. E. (1997). Branch-structure difference in starches of A- and B-type x-ray patterns revealed by their Naegeli dextrins. *Carbohydrate Research, 300*(3), 219-227. http://dx.doi.org/10.1016/s0008-6215(97)00056-6.

Kim, M. J., Choi, S. J., Shin, S. I., Sohn, M. R., Lee, C. J., Kim, Y., Il Cho, W., & Moon, T. W. (2008). Resistant glutarate starch from adlay: Preparation and properties. *Carbohydrate Polymers, 74*(4), 787-796. http://dx.doi.org/10.1016/j.carbpol.2008.04.043.

Kuang, Q., Xu, J., Liang, Y., Xie, F., Tian, F., Zhou, S., & Liu, X. (2017). Lamellar structure change of waxy corn starch during gelatinization by time-resolved synchrotron SAXS. *Food Hydrocolloids, 62*, 43-48. http://dx.doi.org/10.1016/j.foodhyd.2016.07.024.

Lehmann, U., & Robin, F. (2007). Slowly digestible starch – its structure and health implications: a review. *Trends in Food Science & Technology, 18*(7), 346-355. http://dx.doi.org/10.1016/j.tifs.2007.02.009.

Li, J., & Corke, H. (1999). Physicochemical properties of normal and waxy Job's Tears (Coix lachryma-jobi L.) starch. *Cereal chemistry, 76*(3), 413-416.

Liu, X., Zhang, B., Xu, J. H., Mao, D. Z., Yang, Y. J., & Wang, Z. W. (2017). Rapid determination of the crude starch content of Coix seed and comparing the pasting and textural properties of the starches. *Starch-Starke, 69*(1-2). http://dx.doi.org/10.1002/star.201600115.

Lopez-Rubio, A., Flanagan, B. M., Shrestha, A. K., Gidley, M. J., & Gilbert, E. P. (2008). Molecular rearrangement of starch during in vitro digestion: Toward a better understanding of enzyme resistant starch formation in processed starches. *Biomacromolecules, 9*(7), 1951-1958. http://dx.doi.org/10.1021/bm800213h.

Man, J. M., J. W.Cai, Cai, C. H., Xu, B., Huai, H. Y., & Wei, C. X. (2012). Comparison of physicochemical properties of starches from seed and rhizome of lotus. *Carbohydrate Polymers, 88*(2), 676-683. http://dx.doi.org/10.1016/j.carbpol.2012.01.016.

Marcoa, C., & Rosell, C. M. (2008). Effect of different protein isolates and transglutaminase on rice flour properties. *Journal of Food Engineering, 84*(1),

132-139. http://dx.doi.org/10.1016/j.jfoodeng.2007.05.003.

Miao, L., Zhao, S., Zhang, B., Tan, M., Niu, M., Jia, C., & Huang, Q. (2018). Understanding the supramolecular structures and pasting features of adlay seed starches. *Food Hydrocolloids*, 83, 411-418. https://doi.org/10.1016/j.foodhyd.2018.05.034

Pikus, S. (2005). Small-angle X-ray scattering (SAXS) studies of the structure of starch and starch products. *Fibres and Textiles in Eastern Europe*, *13*(5), 82-86.

Qingjie, X. L. H. Z. S. (2012). The Comparison of Job′ s-Tears Powder and Job′ s-Tears Starch on Their Physicochemical Properties and Digestibility [J]. *Journal of the Chinese Cereals and Oils Association*, *7*, 010.

Sandhu, K. S., Singh, N., & Kaur, M. (2004). Characteristics of the different corn types and their grain fractions: physicochemical, thermal, morphological, and rheological properties of starches. *Journal of Food Engineering*, *64*(1), 119-127. http://dx.doi.org/10.1016/j.jfoodeng.2003.09.023.

Scott, P., & Helrich, K. (1990). Official methods of analysis of the Association of Official Analytical Chemists. *Official methods of analysis of the Association of Official Analytical Chemists*.

Singh, N., Singh, J., Kaur, L., Sodhi, N. S., & Gill, B. S. (2003). Morphological, thermal and rheological properties of starches from different botanical sources. *Food Chemistry*, *81*(2), 219-231. http://dx.doi.org/10.1016/S0308-8146(02)00416-8.

Syahariza, Z. A., Sar, S., Hasjim, J., Tizzotti, M. J., & Gilbert, R. G. (2013). The importance of amylose and amylopectin fine structures for starch digestibility in cooked rice grains. *Food Chemistry*, *136*(2), 742-749. http://dx.doi.org/10.1016/j.foodchem.2012.08.053.

Tan, X., Zhang, B., Chen, L., Li, X., Li, L., & Xie, F. (2015). Effect of planetary ball-milling on multi-scale structures and pasting properties of waxy and high-amylose cornstarches. *Innovative Food Science & Emerging Technologies*, *30*, 198-207. http://dx.doi.org/10.1016/j.ifset.2015.03.013.

Tsai, C., Yang, L., & Hsu, H. (1999). Ingestion of adlay may reduce liver fat accumulation in hamsters fed high fat diets. *Food Sci*, *26*, 265-276.

Tseng, Y. H., Yang, J. H., Chang, H. L., Lee, Y. L., & Mau, J. L. (2006). Antioxidant properties of methanolic extracts from monascal adlay. *Food Chemistry*, *97*(3), 375-381. http://dx.doi.org/10.1016/j.foodchem.2005.04.022.

Wang, H., Liu, Y., Chen, L., Li, X., Wang, J., & Xie, F. (2018). Insights into the multi-scale structure and digestibility of heat-moisture treated rice starch. *Food chemistry*, *242*, 323-329. http://dx.doi.org/10.1016/j.foodchem.2017.09.014.

Wenchang, C., Cheng, C. Y., Mengtsan, C., & Kingthom, C. (2000). Effects of dehulled adlay on the culture count of some microbiota and their metabolism in the gastrointestinal tract of rats. *Journal of Agricultural & Food Chemistry*,

526 *48*(3), 829-832. http://dx.doi.org/10.1021/jf990473t.
527 Wu, T. T., Charles, A. L., & Huang, T. C. (2007). Determination of the contents of the
528 main biochemical compounds of Adlay (Coxi lachrymal-jobi). *Food*
529 *Chemistry, 104*(4), 1509-1515.
530 http://dx.doi.org/10.1016/j.foodchem.2007.02.027.
531 Xie, X., Liu, Q., & Cui, S. W. (2006). Studies on the granular structure of resistant
532 starches (type 4) from normal, high amylose and waxy corn starch citrates.
533 *Food Research International, 39*(3), 332-341.
534 http://dx.doi.org/10.1016/j.foodres.2005.08.004.
535 Xu, L., Chen, L., Ali, B., Yang, N., Chen, Y., Wu, F., ... & Xu, X. (2017). Impact of
536 germination on nutritional and physicochemical properties of adlay seed
537 (Coixlachryma-jobi L.). Food chemistry, 229, 312-318.
538 https://doi.org/10.1016/j.foodchem.2017.02.096
539 Yang, S. H., Peng, J., Lui, W. B., & Lin, J. (2008). Effect of adlay species and rice
540 flour ratio on the physicochemical properties and texture characteristic of
541 adlay-based extrudates. *Journal of Food Engineering, 84*(3), 489-494.
542 http://dx.doi.org/10.1016/j.jfoodeng.2007.06.010.
543 Yu, S. F., Ma, Y., Menager, L., & Sun, D. W. (2012). Physicochemical Properties of
544 Starch and Flour from Different Rice Cultivars. *Food and Bioprocess*
545 *Technology, 5*(2), 626-637. http://dx.doi.org/10.1007/s11947-010-0330-8.
546 Zhang, B., Chen, L., Li, X., Li, L., & Zhang, H. (2015). Understanding the multi-scale
547 structure and functional properties of starch modulated by glow-plasma: A
548 structure-functionality relationship. *Food Hydrocolloids, 50,* 228-236.
549 http://dx.doi.org/10.1016/j.foodhyd.2015.05.002.
550 Zhang, G., & Hamaker, B. R. (2009). Slowly digestible starch: concept, mechanism,
551 and proposed extended glycemic index. *Critical Reviews in Food Science and*
552 *Nutrition, 49*(10), 852-867. http://dx.doi.org/10.1080/10408390903372466.
553 Zhu, F. (2017). Coix: Chemical composition and health effects. *Trends in food science*
554 *& technology,* 2017, 61: 160-175. https://doi.org/10.1016/j.tifs.2016.12.003
555

ACCEPTED MANUSCRIPT

Table 1. *Lamellar structural parameters and relative crystallinity of adlay seed starch (AAS), normal maize starch (MS) and potato starch (PS) granules**

Sample	q(nm^{-1})	d	d_L(nm)	d_a	d_c	DC (%)
ASS	0.6624$^{a\#}$	9.48^{c}	9.25^{c}	2.99^{a}	6.26^{c}	35.79^{a}
MS	0.6503^{c}	9.83^{a}	9.61^{a}	2.84^{b}	6.77^{b}	31.25^{b}
PS	0.6528^{b}	9.62^{b}	9.54^{b}	2.59^{c}	6.95^{a}	29.83^{c}

* Parameters obtained by SAXS: q, peak position of semicrystalline lamellae; d, average thickness of semicrystalline lamellae calculated by Woolf-Bragg's equation (d=2π/q). Parameters calculated from one-dimensional correlation function: dL, long repeated distance of semicrystalline lamellae; da, average thickness of amorphous lamellae; dc, average thickness of crystalline lamellae. DC, degree of crystalline of starches obtained from XRD patterns.

Values are means of three determinations (n = 3). Values followed by the different letter within a column differ significantly (*$p < 0.05$).

ACCEPTED MANUSCRIPT

565 **Table 2.** Gelatinization properties parameter for starches

Sample	T_o(°C)	T_p (°C)	T_e (°C)	$T_c - T_o$(°C)	ΔH_{gel} (J/g)
ASS	64.3±0.04c	71.2±0.32a	81.0±0.02a	16.7±0.23a	6.8±0.02c
MS	66.4±0.13a	70.9±0.01b	76.0±0.01b	9.6±0.12c	10.8±0.05b
PS	64.8±0.20b	69.3±0.09c	75.3± 0.12c	10.5±0.08b	12.7±0.02a

566 T_o, on set temperature; T_p, peak temperature; T_e, end temperature; T_e-T_o, gelatinization range; values

567 followed by the different letter within a column differ significantly (*p< 0.05).

ACCEPTED MANUSCRIPT

ACCEPTED MANUSCRIPT

568 **Table 3.** Viscosity characteristics of starches

Sample	Pasting temperatures, °C	Peak viscosities, Bu	Final viscosities, Bu	Breakdown viscosities, Bu	Setback viscosities, Bu
ASS	66.4±0.09$^{b\#}$	1473.0±3.8^{a}	395.0±1.4^{c}	1163.0±2.1^{a}	105.0±0.5^{c}
MS	67.4±0.14^{a}	514.0±3.1^{c}	732.0±1.9^{b}	441.0±1.6^{c}	441.0±0.8^{b}
PS	67.4±0.21^{a}	1191.1±2.3^{b}	1179.0±1.1^{a}	433.0±0.8^{b}	594.0±1.0^{a}

569 $^{\#}$Values followed by the different letter within a column differ significantly (*p< 0.05).

570

ACCEPTED MANUSCRIPT

571 **Table 4.** Digestibility of PS, MS and ASS.

Sample	RDS (%)	SDS (%)	RS (%)
ASS	10.5±1.6[a]	20.6±1.7[a]	68.9±1.1[c]
MS	8.7±0.2[b#]	15.2±1.8[b]	76.0±2.1[b]
PS	4.5±0.6[c]	9.6±0.7[c]	85.9±1.7[a]

572 [#]Values followed by the different letter within a column differ significantly (*p< 0.05).

573

ACCEPTED MANUSCRIPT

ACCEPTED MANUSCRIPT

574 **Figure captions**

575 **Fig.1** X - ray diffraction spectra analysis of different starches

576 **Fig.2** SAXS curves of ASS, MS and PS.

577 **Fig.3** Morphology (SEM: a, c, e; PLM: b, d, f) and size-distribution of starch granules
578 (g). ASS: a b; MS: c, d; PS: e, f. The yellow arrows showed in Figure 3e indicated the
579 channels or pinholes on starch granular surface.

580 **Fig. 4** Structural differences between ASS, MS and PS. d_L, long repeated distance of
581 semicrystalline lamellae; da, average thickness of amorphous lamellae; dc, average
582 thickness of crystalline lamellae. The weak point indicates the α-1,6-glycosidic
583 linkages which cluster in crystalline regions.

584

ACCEPTED MANUSCRIPT

585 **Fig.1**

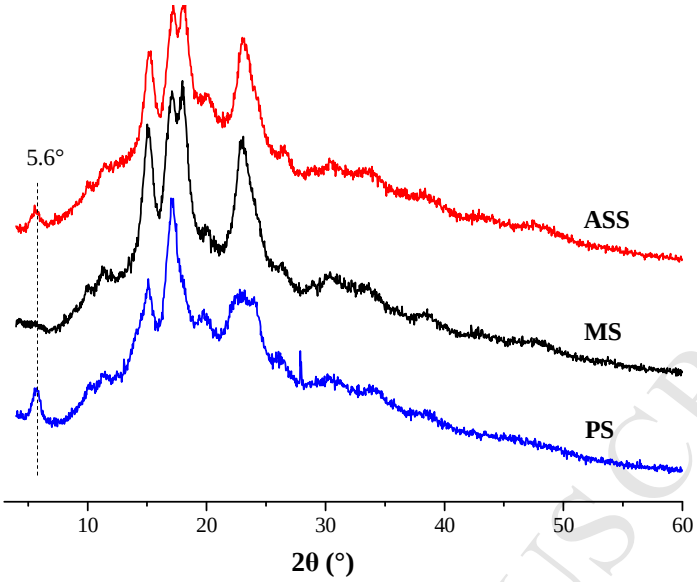

586

587

ACCEPTED MANUSCRIPT

588 **Fig.2**

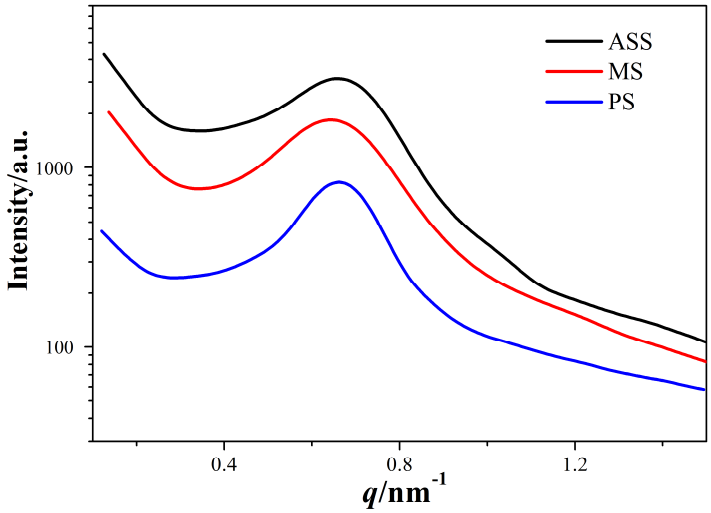

589

590

ACCEPTED MANUSCRIPT

591 **Fig.3**

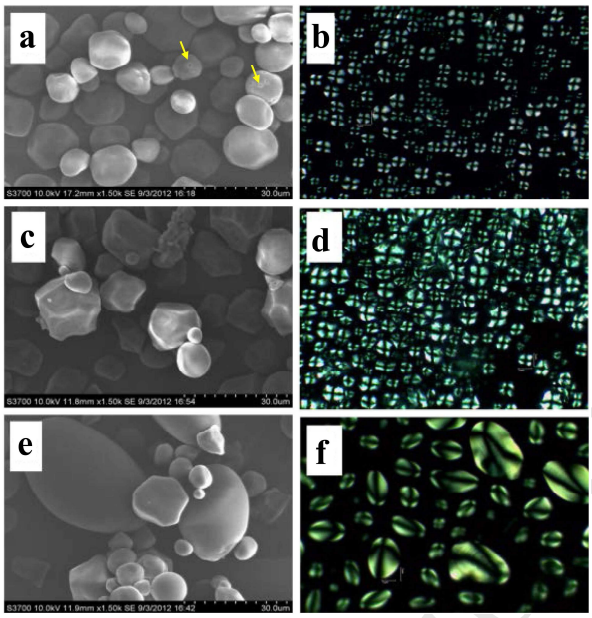

592

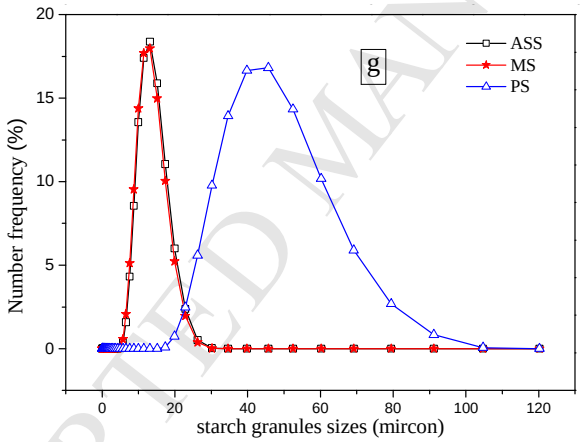

593

594

ACCEPTED MANUSCRIPT

595 **Fig. 4**

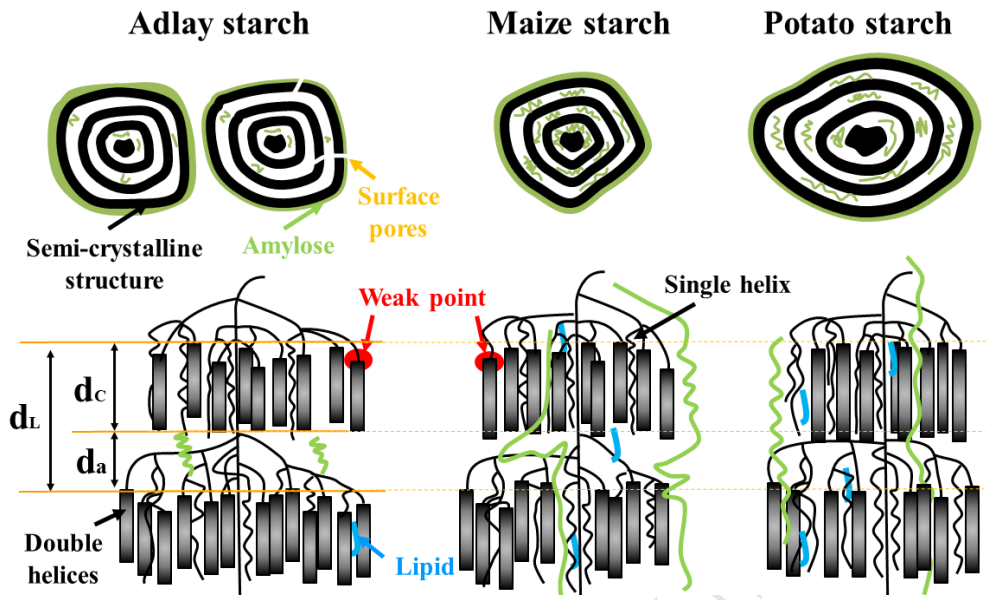

596

ACCEPTED MANUSCRIPT

ACCEPTED MANUSCRIPT

Highlights

- Structural features of adlay seed starch were determined in comparison with normal maize starch and potato starch.
- Great differences were found comparing with normal maize and potato starches.
- Functionalities such as swelling power, solubility, pasting properties and *in vitro* digestibility were investigated.
- Factors determining starches functionalities were discussed.
- A comprehensive elucidation was proposed to reveal the structure-functionalities relationships of starches.

ACCEPTED MANUSCRIPT